Simple wavefield modelling to evaluate the low frequency artifacts in reverse-time migration

John C. Bancroft, CREWES-UofC

Summary

A simplified modelling process was developed to evaluate the low frequency distortion that results from the cross-correlation at the imaging condition in a migration. This distortion must be removed, especially in the case of a full waveform inversion. A one-dimensional model evaluates the movement of multiple reflections and evaluates their effect on the cross correlation and subsequent filtering. Alternative methods of recovering the wavefield prior to the cross-correlation are also evaluated.

Introduction

A Reverse-time migration produces low frequency artifacts that result from the correlation process at the imaging condition (Claerbout 1971) where migrated data coincides with forward modelled data. Figure 1a shows the initial result of a Reverse-time migration of the Marmousi data set, and (b) shows the result after low cut filtering. The low cut filter is shown in (c).

A number of questions about the low frequency noise arise; is it really noise, or could it be some attempt to recover the impedance. Does the low cut filter harm the migration when used in a full waveform inversion (FWI) that attempts to recover the low frequencies of the impedance?

I present a simplified 1D modelling test to address these questions, and to evaluate the algorithms used in the modelling and migration when attempting to recover the reflectivity using Claerbout's method.

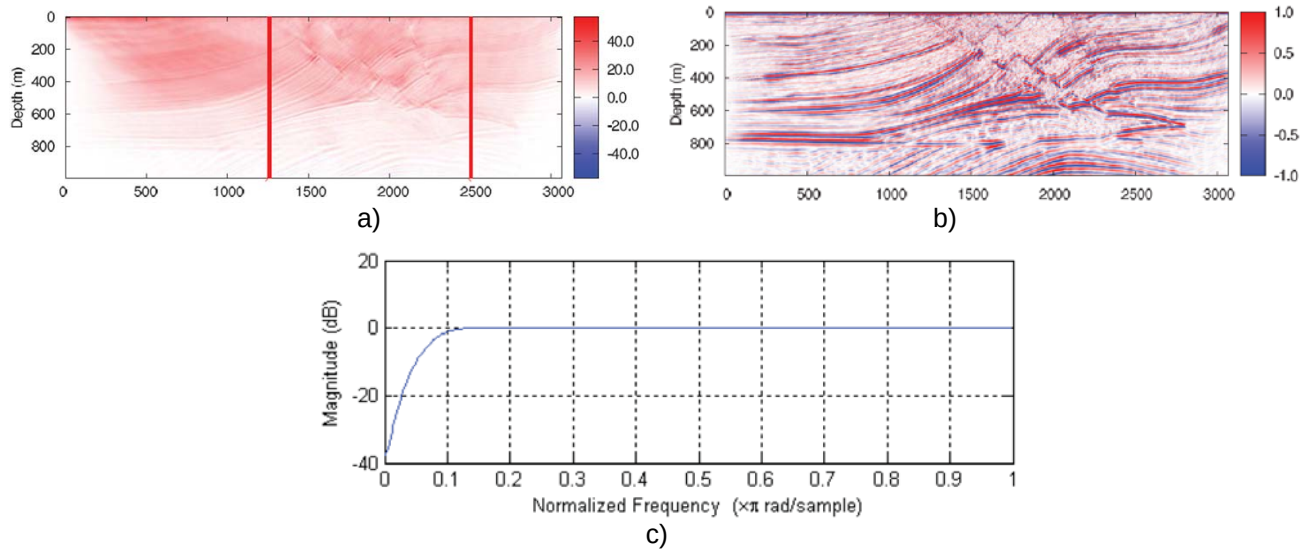

FIG. 1 An example of a) low frequency noise contamination, and b) after a low pass filter was applied, and c) the amplitude spectrum of the filter (Jiang 2010).

Theory and/or Method

I use a very simple model of wavelets moving along a "string" that has three areas with different velocities. Wavelets are reflected from the velocity boundaries and can be absorbed or reflected from the "surface" or the "basement". This simple model would be similar to one seismic trace recorded at the surface vertically above a source location, and where the reflectors are horizontal. The 1D model confines the energy to eliminate spherical divergence.

The wavefield was propagated using a two-way finite difference solution to the acoustic wave equation

$$\frac{\partial^2 P}{\partial z^2} = \frac{1}{v}\frac{\partial^2 P}{\partial t^2}, \tag{1}$$

with the second derivative approximated by (1, -2, 1) giving

$$P_{i-1,j} - 2P_{i,j} + P_{i+1,j} = \frac{\delta z^2}{v^2 \delta t^2}\left(P_{i,j-1} - 2P_{i,j} + P_{i,j+1}\right). \tag{2}$$

where δt and δz are the time and depth sampling increments.

Any outlying element of P can be chosen to be the unknown allowing the wavefield to move in positive or negative time $(i \pm 1)$, for forward or reverse time propagation or down $(j+1)$ for downward continuation. Stability requirements must be met, along with very small sampling increments to prevent grid dispersion. The velocity transitions were also smoothed to eliminate aliasing.

The wavefield may also be propagated using oneway solutions to the wavefield. There are numerous finite different solutions, and variations of the phase shift method (Gazdag 1978). The phase shift method is unconditionally stable for any depth increment, and in the depth-frequency domain (z, ω)

$$P(z + \delta z, \omega) = P(z, \omega) e^{\pm \frac{i \delta z \omega}{v}}. \tag{3}$$

Two initial conditions are required for a two-way solution, but only one is required for a oneway solution. The boundaries may be absorbing or reflective.

Examples

An example of forward modelling is shown in Figure 2, which used the two-way finite difference solution described above. The downward propagating wavelet can be observed along with the primary and multiple reflections. This complete forward model was used to define data at the boundaries.

Figure 3 shows a complete reconstruction of the wavefield by downward continuation using the same finite difference solution. The initial conditions were at depths $z = 0,\ \delta z$, times $t = 0$, and $t = t_{max}$. This figure verifies that a downward continuation can reconstruct the complete wavefield as can reverse time. These initial conditions do not represent the case for surface seismic.

A reconstruction of the wavefield using the reverse time form of the same solution is shown in Figure 4. In this example, only the initial conditions at the surface $z = 0,\ \delta z$ were used, typical of that in a surface seismic application. This is the migrated data that would be used in Claerbout imaging condition.

The forward modelled data used in Claerbout's imaging condition is computed from an estimate of the velocity structure. It could be the same as that in Figure 2, but the data in that figure started with a defined velocity structure and included all multiples. In real data that model is not known.

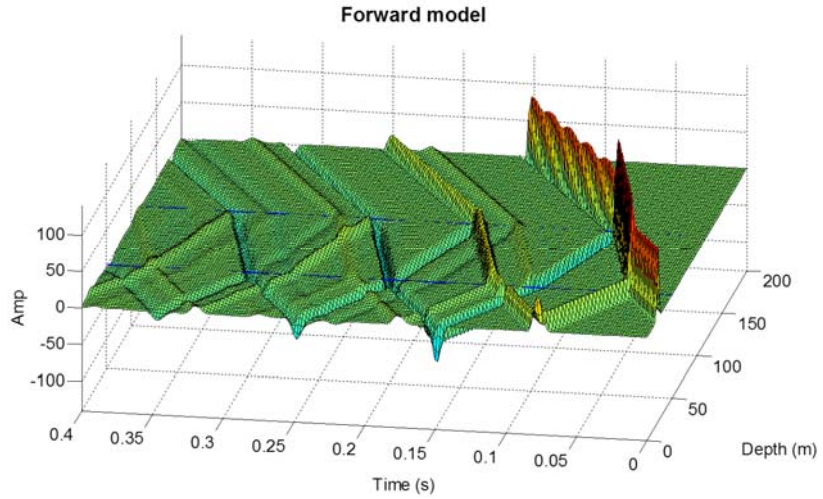

Fig. 2 Forward modelled wavefield using the two-way finite difference solution.

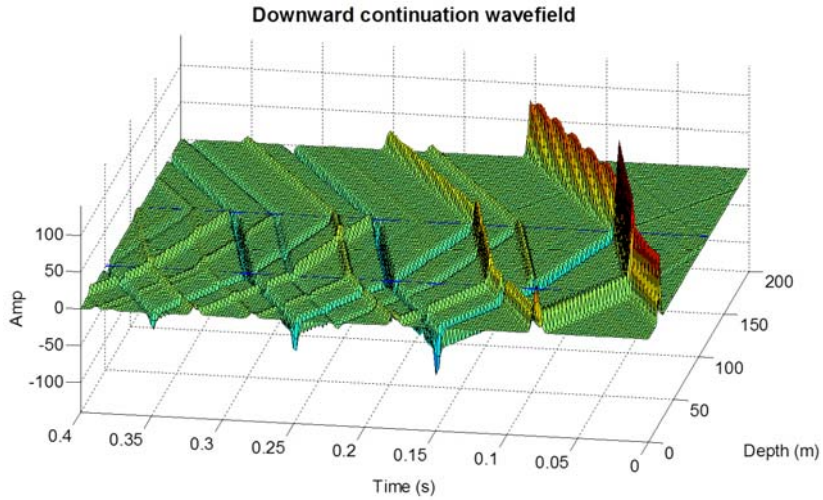

Fig. 3 Reconstructed wavefield using a two-way downward continuation.

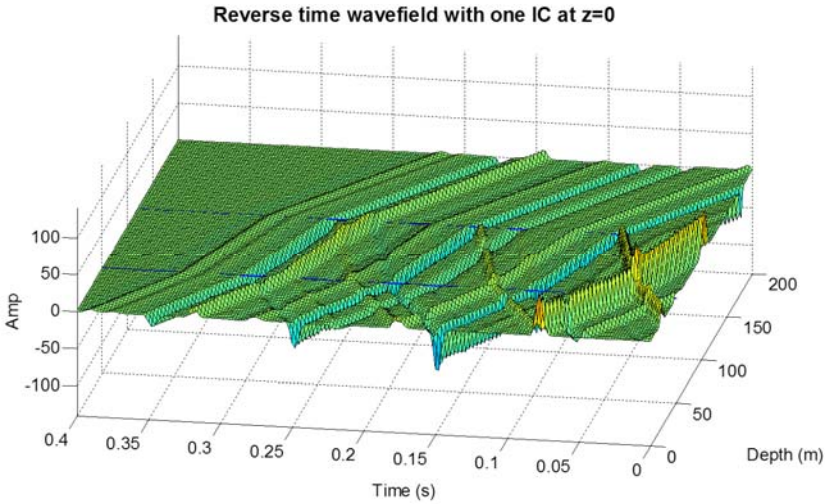

Fig. 4 Reconstructed wavefield using two-way reverse time with one surface IC.

Many reconstructed wavefields were created, and cross-correlations (CC) computed at each time increment. An example of the CC of the forward model (FM) with the fully reconstructed wave reverse-time (RT) wavefield field is shown in Figure 5a that contains low frequency (DC) "contamination" or noise. This "contamination" may be removed using the filter shown in Figure 1a, or with a derivative (-1, 1) to remove the average values. A Laplacian filter (1, -2, 1) may also be used to remove the average value (Liu 2010), but this is also a solution for the second derivative, as used in equation (2). The result of using the derivative is shown in (b) while using a Laplacian results in (c).

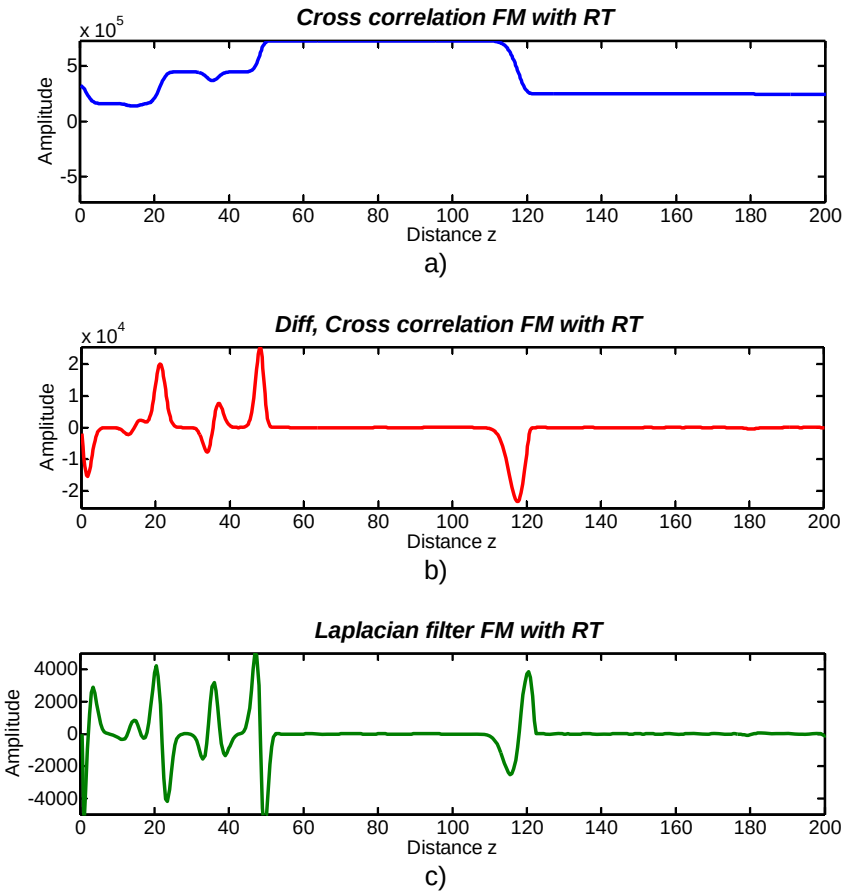

Fig. 5 CC of FM with the fully reconstructed reverse time wavefield, a) the windowed CC, b) differentiated CC, and c) Laplacian filtered CC.

Observations

The low frequency levels (DC) in Figure 5a are similar to, but are not the same as, the velocity profile for the model which is shown in Figure 6. The DC levels at all depths are contaminated by energy from multiple reflections. The forward model used in Figure 5

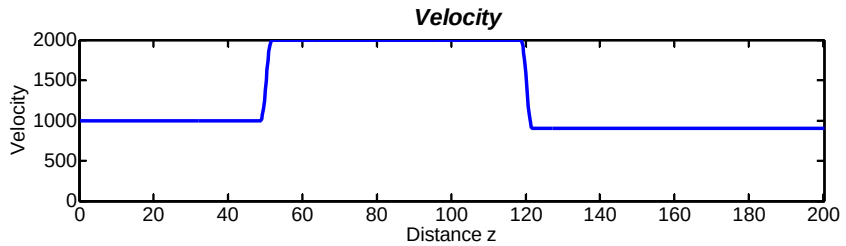

Fig. 6 Velocity array in depth.

Comments and Conclusions

The forward modelled wavefield can be reconstructed using reverse time or downward continuation solutions to the wave-equation.

The DC contamination in the cross-correlations appears to be related to the impedance of the model when using the fully reconstructed wavefield. This reconstructed wavefield cannot be created using surface seismic.

The derivative and Laplacian filters distort the shape of the recovered wavelets.

The reverse time method does not recover the full wavefield.

After many tests using different algorithms, the two-way reverse time method did not show improved results over one-way methods.

Two-way finite difference solutions require two ICs. Only one is recorded at the surface $z = 0$. The second IC at $z = \delta z$ is computed by time shifting the surface IC towards $t = 0$. This is similar to a oneway propagation using the single surface IC.

The two-way reverse time migration creates multiples that are different from those of a forward model.

A reverse-time migration requires the full wavefield to be computed and save prior to any CC. Only the zero lag cross-correlation point can be computed during the reverse time process.

A downward continuation algorithm can compute the cross correlation at each downward step.

The inclusion of the multiples in the reconstruction of the wavefield did not add to the accuracy when estimating the reflectivity.

Removal of multiples (as in standard processing) may provide a superior estimate of the reflectivity.

Oneway forward modelling may produce superior reflectivities as it eliminates multiples.

The mathematical theory of full waveform inversion (FWI) dictated the requirement of a reverse time migration and a cross correlation with a forward model. Recent work by Margrave et al. (2010, 2011, and 2012) indicates that alternative migration algorithms can be used successfully with FWI.

Full waveform inversing using a time migration has been successfully demonstrated, (Khaniani et al. 2013).

This work used a simplified 1D model. Further testing with multi-dimensional models is required to verify these initial observations.

Acknowledgements

I thank the sponsors of the CREWES project for supporting this work.

References

Bancroft, J. C., 2013, Comments on wavefield propagation using Reverse-time and Downward continuation, CREWES Research Report, Vol. 25.

Claerbout, J. F., 1971, Toward a unified theory of reflector mapping, Geophysics, 36, No. 3, 467-481.

Gazdag, J., 1978, Wave equation migration with the phase shift method, Geophysics, Vol. 43, 1342 – 1351.

Khaniani, H., Bancroft, J. C., and Von Lumen, E., 2013, Iterative multiparameter elastic waveform inversion using prestack Kirchhoff approximation, CREWES Research Report, Vol. 25.

Liu, H, Zou, Z., and Cui, Y., 2010, Denoising and storage in seismic reverse time migration, Chinese Journal of Geophysics, Vol. 53, N0. 5, 828 – 837.

Margrave, G F., K. Innanen, and M. Yedlin, 2012, A Perspective on Full Waveform Inversion, CREWES Research Report, Vol. 24.

Margrave, G F., M. Yedlin, and K. Innanen, 2011, Full waveform inversion and the inverse Hessian, CREWES Research Report, Vol. 23.

Margrave, G F., R. Ferguson, and C. M. Hogan, 2010, Full waveform inversion with wave equation migration and well control, CREWES Research Report, Vol. 22.

Zaiming Jiang, 2012, Elastic wave modelling and reverse time migration by staggered grid finite difference method, PhD Dissertation, Department of Geoscience, University of Calgary.